Enhancing In Vivo Preclinical Studies with VivoVist™ and Photon-Counting Micro-CT Imaging

C. T. Badea[1], A. Rickard[2], A. Allphin[1], D. P. Clark[1], K. B. Ghaghada[3], S. Ridwan[4], H. Smilowitz[4], J. F. Hainfeld[5], Y. M. Mowery[2]

[1]Quantitative Imaging and Analysis Lab, Department of Radiology, Duke University Medical Center, Durham, NC 27710, USA
[2]Department of Radiation Oncology, Duke University Medical Center, Durham, NC 27710, USA
[3]E. B. Singleton Department of Radiology, Texas Children's Hospital/Baylor College of Medicine, Houston, TX 77030, USA,
[4]Department of Cell Biology, UConn Health, Farmington, CT 06030, USA
[5]Nanoprobes, Inc.

ABSTRACT

This study investigated the application of VivoVist™, a high-contrast micro-CT contrast agent, in spectral photon-counting (PC) micro-CT imaging in mouse models. With a long blood half-life, superior concentration, and reduced toxicity VivoVist, composed of barium (Ba)-based nanoparticles, offers a cost-effective solution for enhancing computed tomography (CT) imaging. To evaluate its efficacy, we employed an in-house developed spectral micro-CT with a photon-counting detector. VivoVist was administered through retro-orbital injection in a non-tumor-bearing C57BL/6 mouse and in two mice with MOC2 buccal tumors, with scans taken at various post-injection intervals. We used a multi-channel iterative reconstruction algorithm to provide multi-energy tomographic images with a voxel size of 125 microns or 75 microns for high-resolution scans; we performed post-reconstruction spectral decomposition with water, calcium (Ca), iodine (I), and barium (Ba) as bases. Our results revealed effective separation of Ba from I-based contrast agents with minimal cross-contamination and superior contrast enhancement for VivoVist at 39 keV. We also observed VivoVist's potential in delineating vasculature in the brain and its decreasing concentration in the blood over time post-injection, with increased uptake in the liver and spleen. We also explored the simultaneous use of VivoVist and liposomal iodinated nanoparticles in a cancer study involving radiation therapy. Our findings reveal that VivoVist, combined with radiation therapy, did not significantly increase liposomal iodine accumulation within head and neck squamous cell carcinoma tumors. In conclusion, our work confirms VivoVist's promising role in enhancing PCCT imaging and its potential in studying combination therapy, warranting further investigation into its applications in diagnostics and radiotherapy.

Keywords: x-ray CT (CT), small animal imaging (SMAX), photon counting
*cristian.badea@duke.edu; phone 1-919-684-7509; https://sites.duke.edu/qial/

1. INTRODUCTION

Computed Tomography (CT) has revolutionized medical imaging with its ability to provide high-resolution anatomical details. However, its efficacy in contrast resolution remains limited when using traditional energy-integrating detectors (EID). The advent of spectral photon-counting detectors (PCD) marks a significant advancement in CT technology, offering enhanced contrast capabilities and enabling material-specific imaging through quantitative material separation in a single scan [1]. Our research group has been at the forefront of pioneering preclinical photon counting (PC)CT, developing prototypes and showcasing their utility in diverse areas such as cancer [2] and cardiac imaging in mice [3].

In the realm of contrast agents, nanoparticles have emerged as game-changers, especially for micro-CT imaging. For small animal studies, there is a growing demand for blood pool contrast agents that provide prolonged circulation time and stable enhancement. Elements like iodine (I), gold (Au), and barium (Ba) are increasingly favored due to their excellent X-ray attenuation properties and biocompatibility [4]. Among these, barium-based nanoparticles such as VivoVist (Nanoprobes,

Medical Imaging 2024: Clinical and Biomedical Imaging, edited by Barjor S. Gimi, Andrzej Krol, Proc. of SPIE Vol. 12930, 129300V · © 2024 SPIE
1605-7422 · doi: 10.1117/12.3005892

Inc: https://www.nanoprobes.com/), shows exceptional promise. VivoVist stands out for its extended blood half-life, high contrast efficiency, and cost-effectiveness, making it a valuable tool in enhancing CT imaging quality. However, the potential of VivoVist in conjunction with spectral PC micro-CT imaging remains relatively unexplored. This paper aims to evaluate VivoVist using spectral PC micro-CT imaging and its applications in cancer studies in small animals.

2. METHODS

2.1 VivoVist™

VivoVist™ is a commercially available micro-CT contrast agent. According to the manufacturer, the barium (Ba)-based nanoparticles constituting VivoVist measure approximately 136 nm, with a concentration of 300 mg/ml. The blood half-life for VivoVist is ~14 hours in mice.

2.2 PCCT Scanning

For this study, we used a spectral micro-CT system comprising two imaging chains: one for energy integration and another for photon counting, as detailed in our previous research [5]. Each chain is equipped with a G-297 X-ray tube (Varian Medical Systems, Palo Alto, CA) featuring a 0.3 mm focal spot size and powered by an Epsilon high-frequency X-ray generator (EMD Technologies, Quebec, Canada). We specifically employed the photon counting chain, equipped with a SANTIS 1604 CdTe-based photon counting detector (PCD) developed by DECTRIS, Ltd. This PCD features a 150 µm pixel size and four energy thresholds, allowing for optimized spectral imaging.

The source-to-detector and source-to-object distances were set at 831 and 680 mm, respectively, yielding approximately 1.2x geometric magnification at the detector. The imaging subjects, both phantoms and mice injected with VivoVist™, were positioned on a translational stage. Scanning was conducted via a helical trajectory, translating 1.25 cm over three rotations. This approach expanded the field-of-view along the z-axis and helped reduce ring artifacts in the reconstructed images. The scanning parameters were set at 80 kVp and 4 mA. We collected 900 projections, each with an exposure duration of 200 ms. The PCD thresholds (25, 34, 39, 50 keV) were chosen to optimize contrast agent differentiation from bone, i.e., Calcium (Ca), soft tissue (primarily water, H_2O), iodine (I) (the most commonly used material in CT contrast agents, K-edge at 33.2 keV), and Ba (K-edge at 37.4 keV).

Additionally, we obtained a higher resolution scan using a microfocus X-ray tube (L9181-02 39W; Hamamatsu; tungsten anode; filtration: 0.50 mm beryllium; 16-50 µm spot size), where the geometric magnification was increased to ~2x by adjusting the source-to-detector distance. The same PCD detector was used for the high resolution scan. The high resolution scan was reconstructed with 75 µm.

2.3 Reconstruction and material decomposition

The PCCT data were jointly reconstructed using a multi-channel iterative algorithm and an isotropic voxel size of 125 µm or 75 µm (for a higher resolution scan). Specifically, we applied the split Bregman method with the add-residual-back strategy [6] and rank-sparse kernel regression regularization (RSKR [7]) implemented in our open source MCR Toolkit[8]. We performed image-based material decomposition on PC iterative reconstructions using the method of Alvarez and Macovski [9] extended to include K-edge materials. Thus, we performed a post-reconstruction spectral decomposition with H_2O, Ca, and two K-edge materials, M_i, (i.e., I and Ba) as bases: $X(e) = C_{H2O}M_{H2O}(e) + C_{Ca}M_{Ca}(e) + \sum_{i=1}^{2} C_i M_i(e)$. In this formulation, M is a matrix of material sensitivities at each energy. We computed these values by fitting the slope of attenuation measurements taken in material vials of known material concentrations. C is the concentration in mg/mL of each material. Finally, X is the attenuation coefficient of the voxel under consideration at energy (e). Material decomposition was performed by matrix inversion, solving the following linear system at each voxel: $\mathrm{C} = \mathrm{X}\mathrm{M}^{-1}$. Orthogonal subspace projection was used to prevent negative concentrations [7]. Post-decomposition, the material maps in color were combined and visualized in ImageJ.

2.4 Small animal imaging and VivoVist evaluation

In our preliminary phase, we evaluated VivoVist in a non-tumor-bearing C57BL/6 mouse, administering VivoVist via retro-orbital injection (0.2 ml/25 g mouse) to deliver approximately 60 mg of Barium. We conducted scans at intervals of 20 minutes, 2 hours, and 4 hours after the injection to monitor the distribution and clearance of VivoVist.

For our cancer-specific study, we utilized an orthotopic MOC2 model of head and neck squamous cell carcinoma (HNSCC) in mice. Tumors were induced by submucosal injection of 30,000 MOC2 cells into the buccal mucosa **[10]**. Mice were randomized into two groups: i) the test group (n=5) received VivoVist (0.15 ml/25 g mouse) via retro-orbital injection on day 0, while ii) the control group (n=4) did not receive VivoVist. On the following day, all mice underwent a 20 Gy dose of radiation therapy (RT) using the Xstrahl small animal radiation research platform (SARRP) for precise targeting.

Subsequently, one day post-RT, we administered liposomal iodine (Lip-I) nanoparticles (0.3 ml/25 g mouse) to all mice. Lip-I, with an Iodine concentration of 110 ± 4 mg/ml and an average liposome size of 145 ± 6 nm, was used as an imaging surrogate for liposomal chemotherapeutics like Doxil. This approach aligns with our previous work on using liposomal nanoparticles for spectral PCCT-based functional imaging of tumor vasculature[2]. Imaging of the tumors was performed on day 5, three days after Lip-I injection, to assess the enhanced permeability and retention (EPR) effect **[11]**, which can be increased via RT **[12]**. The study aimed to demonstrate the effectiveness of spectral PCCT imaging in differentiating Iodine and Barium nanoparticles within tumor tissues. Moreover, this exploratory study investigates the potential of combining VivoVist with Lip-I and PCCT to enhance RT effects. Both Iodine and Barium are high atomic number (Z) elements that can potentially intensify the local RT dose delivered to tumor vasculature, thereby increasing vascular disruption and improving the delivery of liposomal chemotherapeutics. Our platform, with Lip-I as an imaging surrogate, offers a promising approach to test and optimize combination treatments involving liposomal cisplatin or Doxil.

2.5 Analysis

After decomposition, we utilized the lowest energy PCCT images at 25 keV for tumor segmentation, excluding bone, using ITK-SNAP (http://www.itksnap.org). This process generated a binary mask that provided a measure of tumor volume. This mask was then imported into Matlab (MathWorks, MA) along with Barium (Ba) and Iodine (I) material maps. The binary mask was applied to the decomposition maps, ensuring that only tumor voxels were analyzed. The I maps were used to measure the average concentrations of I higher than 0.5 mg/ml in the tumors. A threshold of 0.5 mg/ml was chosen due to detection limits. We also quantified the tumor fraction containing I, the total I mass, and average I concentration in tumors. A t-test was performed to identify statistically significant differences ($p<0.05$) between the control and test groups.

3. RESULTS

PCCT images captured over the thorax of a C57BL/6 mouse across four energy levels, along with their material decomposition, are displayed in Fig.1.

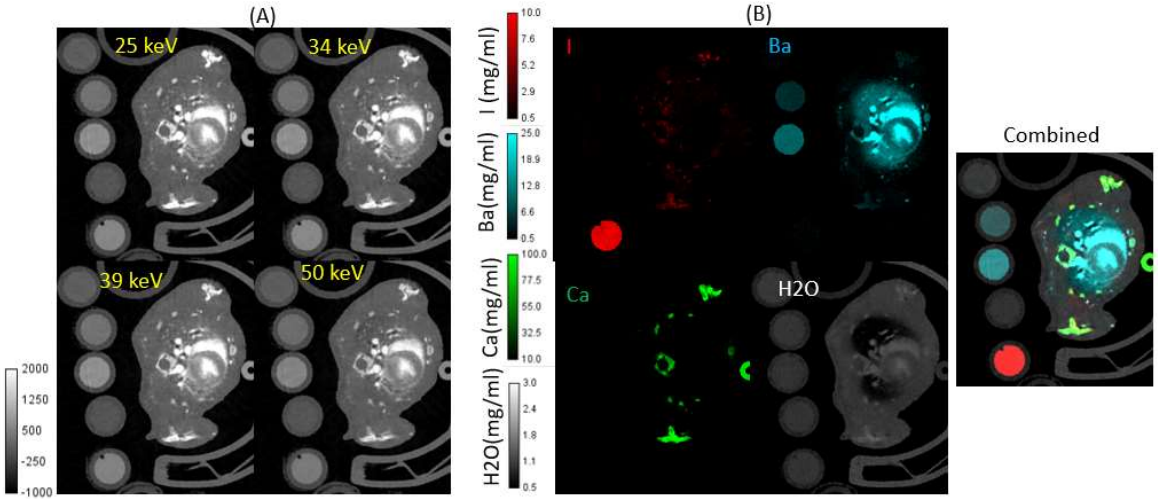

Fig.1: PC micro-CT in an axial orientation of a mouse thorax at 4 threshold energies (25, 34, 39, 50 keV) (left) and the material decomposition maps corresponding to I, Ca, H_2O and Ba (right). The calibration vial of I was 10 mg/ml, and the two Ba vials were 6 and 3 mg/ml. No iodine-based contrast agent was injected in this animal.

Calibration vials containing I, Ba, Ca and H_2O are also visible. The partitioning of iodine (I) and barium (Ba) is clearly effective despite the proximity of their K-edges (33.2 (I) and 37.4 keV (Ba)), displaying negligible cross-contamination between the two material maps. Slight cross-contamination is observable in the water (H_2O) material map with some Ba residuals, but no Ba-I contamination is visible. This is remarkable considering the proximity of the two K-edges of I (33.2 keV) and Ba (37.4 keV).

Fig.2 (A) presents the enhancement in HU for the scan conducted 20 minutes after the injection of VivoVist. It is noteworthy that the 39 keV threshold image demonstrates the highest enhancement (exceeding 2000 HU in blood), given its alignment with the K-edge of Ba. In Fig. 2B, we illustrate the contrast evolution for the same organs at 20 minutes, 2 hours, and 4 hours post-injection of VivoVist. The scans show diminishing contrast in the blood and increased uptake by the liver and spleen, which consequently appear brighter.

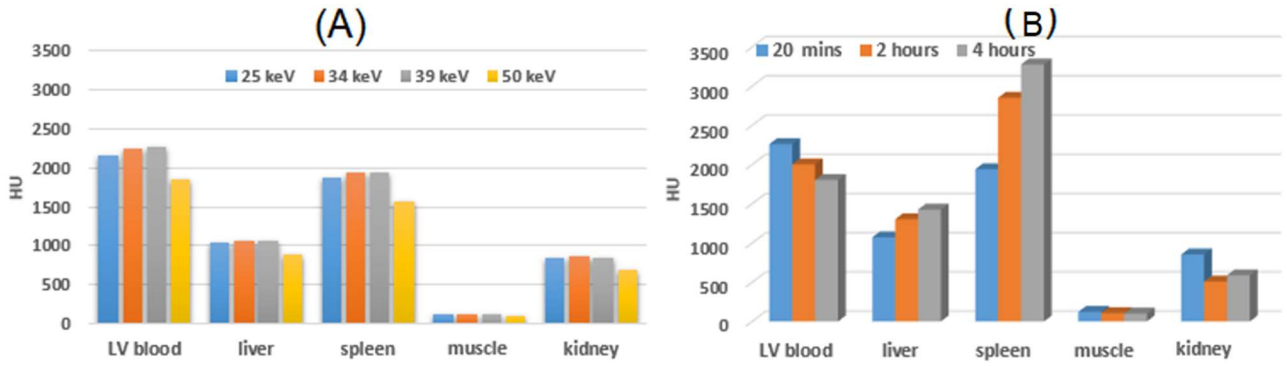

Fig.2: A) Enhancement in HU at the 4 energy thresholds for various organs in the body in a scan at 20 minutes post VivoVist injection. Note the higher peak at 39 keV. B) The bio-distribution at the 20 minute, 2 hour and 4 hour post-injection imaging time points for the 39 keV threshold image. LV refers to left ventricle.

Fig.3 displays the vascular imaging capabilities offered by VivoVist with the higher resolution scan (i.e., at 75 µm) acquired at 30 minutes post injection. This scan proves valuable particularly in delineating small vessels, such as those found in the mouse brain.

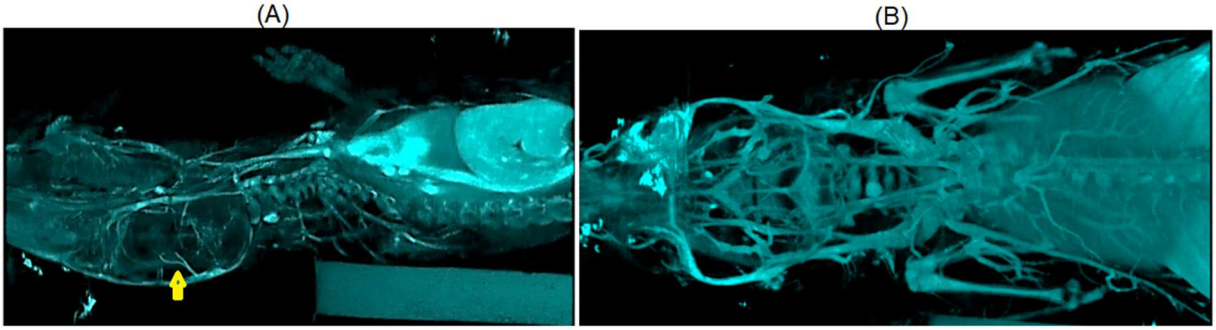

Fig.3: 3D rendering of the mouse vasculature in the upper body using the 75 µm data set in sagittal (A) and coronal (B) views. Note that vasculature in the brain is clearly visible (arrow).

Fig. 4 displays the spectral decomposition maps for Iodine (I), Barium (Ba), Calcium (Ca), and Water (H_2O) in mice with HNSCC tumors, delineated by ellipsoids. These images were captured using photon counting CT (PCCT) on day 5. Notably, the control mouse, which did not receive VivoVist, shows an absence of Barium in its spectral map, whereas the test mouse demonstrates Ba presence. In both cases, there is evidence of Iodine accumulation within the tumor regions. In the test group, there is a partial overlapping presence of the two nanoparticle types.

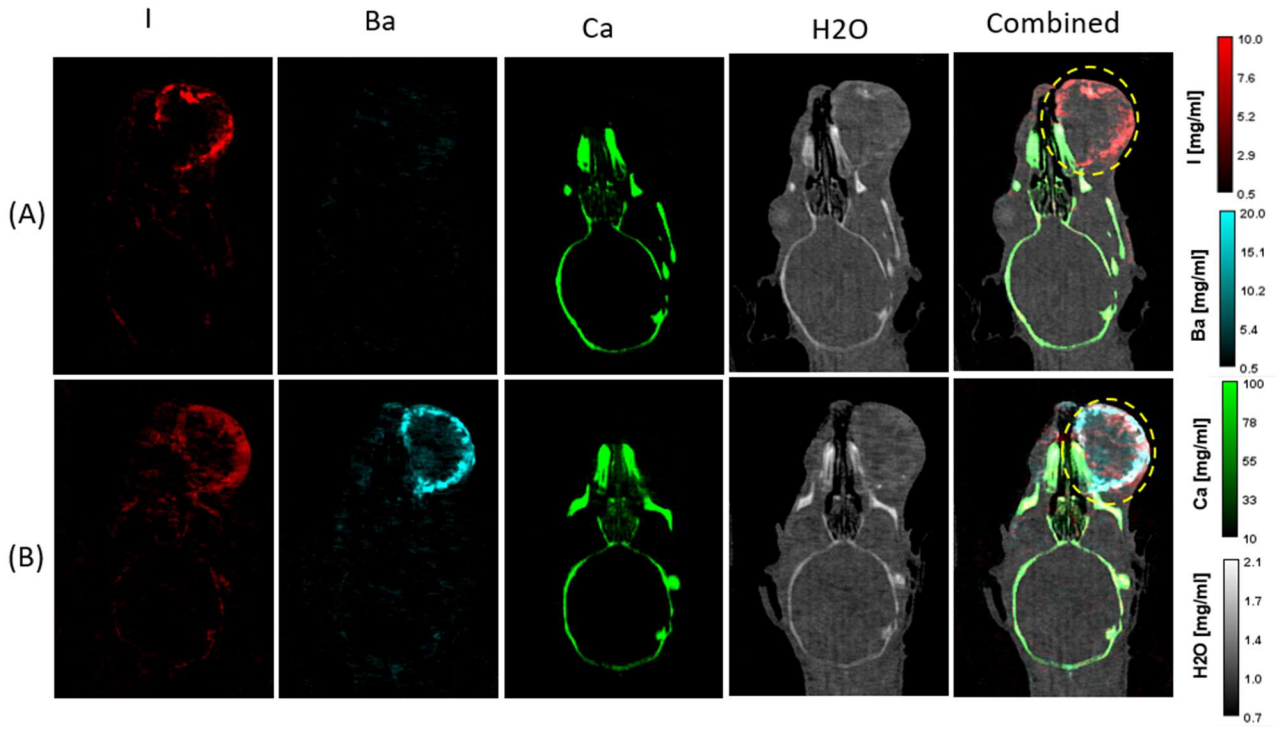

Fig. 4: The spectral decomposition maps corresponding to I, Ba, Ca and H2O in mice with HNSCC tumors (ellipsoids) and imaged with PCCT at day 5. We show mice from the control (A) and test (B) groups. The control mouse has not received VivoVist and consequently the Ba map appears empty. In both mice, I accumulation in the tumor is demonstrated. The color bars show the concentration of each material in the decomposition in mg/ml.

Fig.5 compares the tumor volumes and the iodine-based quantitative measures in the test and control groups. The test group (VivoVist + RT + Lip-I) showed a significantly larger average tumor volume (0.31 ml) compared to the control group (0.2 ml) ($p = 0.011$). This indicates a statistically significant difference in tumor size between the two groups. The Iodine Tumor Volume Fraction, which measures the fraction of the tumor volume containing detectable Iodine, was lower in the test group (64.80%) compared to the control group (74.62%). This difference was not statistically significant ($p = 0.08$). This indicates that, despite the larger tumor sizes in the test group, the proportion of tumor with detectable Iodine was not significantly different from the control group.

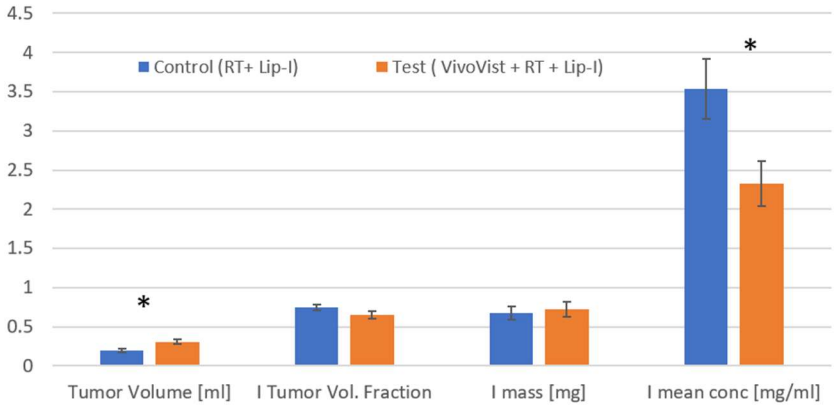

Fig.5: Comparison of tumor volumes, I tumor volume fraction, I mass and I mean concentration in tumors for VivoVist + RT treated mice (n=5) and control mice (n=4). * demonstrates a statistically significant difference ($p<0.05$) between test and control groups. Error bars represent standard error of the mean.

The accumulated Iodine mass within the tumors was slightly higher in the test group (0.72 mg) compared to the control group (0.67 mg), but this difference was not statistically significant ($p = 0.37$). This suggests that the overall accumulation of Iodine in the tumors was similar between the two groups. The mean concentration of Iodine in the tumors was significantly lower in the test group (2.32 mg/ml) compared to the control group (3.53 mg/ml) ($p = 0.017$). This significant difference indicates that, on average, the tumors in the test group had a lower concentration of Iodine. This could suggest that VivoVist + RT does not enhance the Lip-I accumulation within the HNSCC tumors. These findings could have implications for the use of high Z elements such as BaNp in combination with RT and liposomal chemotherapeutics (such as Doxil) in treating tumors.

4. DISCUSSION AND CONCLUSIONS

Our study introduced VivoVist as a contrast agent in spectral PCCT imaging in mouse models. The results demonstrate VivoVist's effectiveness in enhancing contrast (>2000 HU in the blood at 20 minutes post-injection). The distinct K-edge of barium (37.4 keV) within VivoVist can be used by PCCT for separation from other elements, notably Iodine, in spectral decomposition, minimizing cross-contamination and highlighting its potential for detailed material mapping in complex biological environments. Furthermore, the imaging capabilities demonstrated in Fig. 3, particularly at a higher resolution of 75 μm, underscore VivoVist's utility in delineating small vessels, such as those in the mouse brain. The prolonged blood half-life of VivoVist, estimated at around 14 hours, is a notable advantage for extended imaging studies. This feature facilitates sustained and stable visualization of vascular structures, which is invaluable in tracking physiological processes or monitoring pathological progression over time.

In our cancer study, we tested VivoVist's potential to augment the effectiveness of radiotherapy in a radioresistant orthotopic HNSCC mouse model. Barium's high atomic number suggests a potential role in enhancing radiation dose delivery to targeted areas, akin to the use of gold or iodine nanoparticles in radiotherapy[13-17]. This property could be important in refining treatment strategies, including for vascular disruption. The study's findings, particularly shown in Figs. 4 and 5, reveal that VivoVist and RT did not necessarily increase Lip-I accumulation within HNSCC tumors. The test group, treated with VivoVist + RT + Lip-I, showed larger tumor volumes and lower mean concentration of iodine compared to the control group. However, we acknowledge that our findings are based on a small study with a very limited number of mice. Additional mice and histologic validation would be also required to understand better the distribution of VivoVist and Lip-I and the vascular distribution in the two groups.

In conclusion, our research establishes VivoVist as a potent contrast agent for spectral PC micro-CT imaging, offering significant contrast enhancement and prolonged bloodstream presence. Its ability to distinctly map barium and iodine in complex biological structures is crucial for material differentiation in diagnostic imaging. Future research should explore VivoVist's broader applications in diagnostics and radiotherapy, its safety profile for intravascular use, and its interactions with other therapeutic agents. Integrating VivoVist into a wider range of diagnostic and treatment modalities could significantly advance spectral PCCT imaging and targeted therapeutic interventions.

5. ACKNOWLEDGEMENTS

All work was performed at the Quantitative Imaging and Analysis Lab supported by the NIH National Cancer and National Aging Institutes (R01 CA196667, U24 CA220245, RF1AG070149). We acknowledge the help of Dr. Yi Qi with the animal experiments.

6. CONFLICTS OF INTEREST

K.B.G is a research consultant for Alzeca Biosciences LLC.

REFERENCES

1. Taguchi, K. and J.S. Iwanczyk, *Vision 20/20: Single photon counting x-ray detectors in medical imaging.* Med Phys, 2013. **40**(10): p. 100901.
2. Badea, C.T., et al., *Functional imaging of tumor vasculature using iodine and gadolinium-based nanoparticle contrast agents: a comparison of spectral micro-CT using energy integrating and photon counting detectors.* Phys Med Biol, 2019. **64**(6): p. 065007.
3. Clark, D.P., M. Holbrook, C.L. Lee, and C.T. Badea, *Photon-counting cine-cardiac CT in the mouse.* PLoS One, 2019. **14**(9): p. e0218417.
4. Clark, D.P. and C.T. Badea, *Advances in micro-CT imaging of small animals.* Phys Med, 2021. **88**: p. 175-192.
5. Holbrook, M.D., D.P. Clark, and C.T. Badea, *Dual source hybrid spectral micro-CT using an energy-integrating and a photon-counting detector.* Phys Med Biol, 2020. **65**(20): p. 205012.
6. Gao, H., H. Yu, S. Osher, and G. Wang, *Multi-energy CT based on a prior rank, intensity and sparsity model (PRISM).* Inverse Probl, 2011. **27**(11): p. 115012.
7. Clark, D.P. and C.T. Badea, *Hybrid spectral CT reconstruction.* PLOS ONE, 2017. **12**(7): p. e0180324.
8. Clark, D.P. and C.T. Badea, *MCR toolkit: A GPU-based toolkit for multi-channel reconstruction of preclinical and clinical x-ray CT data.* Med Phys, 2023. **50**(8): p. 4775-4796.
9. Alvarez, R.E. and A. Macovski, *Energy-selective reconstructions in X-ray computerized tomography.* Phys Med Biol, 1976. **21**(5): p. 733-44.
10. Judd, N.P., et al., *ERK1/2 regulation of CD44 modulates oral cancer aggressiveness.* Cancer Res, 2012. **72**(1): p. 365-74.
11. Maeda, H., *The enhanced permeability and retention (EPR) effect in tumor vasculature: the key role of tumor-selective macromolecular drug targeting.* Adv Enzyme Regul, 2001. **41**: p. 189-207.
12. Moding, E.J., et al., *Dual-energy micro-computed tomography imaging of radiation-induced vascular changes in primary mouse sarcomas.* Int J Radiat Oncol Biol Phys, 2013. **85**(5): p. 1353-9.
13. Hainfeld, J.F., F.A. Dilmanian, D.N. Slatkin, and H.M. Smilowitz, *Radiotherapy enhancement with gold nanoparticles.* J Pharm Pharmacol, 2008. **60**(8): p. 977-85.
14. Hainfeld, J.F.e.a., *Gold nanoparticle imaging and radiotherapy of brain tumors in mice.* Nanomedicine, 2013. **8**(10): p. 1601-1609 Here is the list of references you provided, formatted in the Refer/BibIX format:.
15. Ashton, J.R., et al., *Dual-Energy CT Imaging of Tumor Liposome Delivery After Gold Nanoparticle-Augmented Radiation Therapy.* Theranostics, 2018. **8**(7): p. 1782-1797.
16. Hainfeld, J.F., et al., *Iodine nanoparticles enhance radiotherapy of intracerebral human glioma in mice and increase efficacy of chemotherapy.* Sci Rep, 2019. **9**(1): p. 4505.
17. Badea, C., et al. *A spectral CT study on iodine augmentation of radiation therapy and its potential for combination with chemotherapy*. in *Medical Imaging 2020: Biomedical Applications in Molecular, Structural, and Functional Imaging*. 2020. International Society for Optics and Photonics. 113171N